X-ray crystal structure of a locked nucleic acid (LNA) duplex composed of a palindromic 10-mer DNA strand containing one LNA thymine monomer†

Martin Egli,[*a] **George Minasov,**[b] **Marianna Teplova,**[a] **Ravindra Kumar**[c] **and Jesper Wengel**[c]

[a] *Department of Biological Sciences, Vanderbilt University, Nashville, Tennessee 37235, USA,*
E-mail: martin.egli@vanderbilt.edu

[b] *Department of Molecular Pharmacology and Biological Chemistry, Northwestern University Medical School,*
Chicago, Illinois 60611, USA

[c] *Department of Chemistry, University of Southern Denmark, DK-5230 Odense M, Denmark*

Locked nucleic acid (LNA), a recently introduced nucleic acid analogue with a bicyclic 2′-O,4′-C-methylene linked furanose sugar, exhibits enhanced affinities for DNA and RNA relative to the corresponding oligodeoxyribonucleotides and oligoribonucleotides; we report the first crystal structure of an LNA unit incorporated in an oligonucleotide duplex. The structure at 1.4 Å resolution of the DNA–LNA decamer duplex with one LNA thymine monomer per strand provides a detailed view of the conformation and hydration of locked nucleic acid residues in a duplex A-form.

LNA (Fig. 1), exhibits stability of self-pairing that significantly exceeds those observed with DNA and RNA.[1–3] The UV melting temperatures of mixed DNA–LNA[1,4] and RNA–LNA[5] strands paired to DNA or RNA are increased by between 4 to 9 °C per modified residue compared to the corresponding unmodified duplexes. Increased RNA affinity, higher nuclease resistance and the observation that RNAs targeted by mixed DNA–LNA oligonucleotides are degraded by RNase H render LNA a promising third-generation antisense modification.[6]
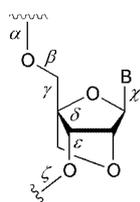
Fig. 1 Structure of LNA; torsion angles are labeled.

NMR solution structures of DNA–LNA[7–9] and RNA–LNA[10] duplexes containing either single or multiple LNA residues in one strand demonstrated the preference of the locked sugar for a C3′-endo conformation. Based on these experiments it was concluded that enthalpic (improved stacking) and entropic factors (conformational preorganization) may account for the unprecedented gains in the thermodynamic stabilities of LNA-modified duplexes. In order to examine the detailed conformation of LNA residues and the hydration of the bicyclic sugar moiety, we determined the single crystal structure of the DNA–LNA decamer duplex [GCGTAT^{L}ACGC]$_2$ with a single LNA thymine T^L at high resolution.

The mixed DNA–LNA decamer was synthesized‡ using phosphoramidite chemistry as previously described[1] and purified to >98%. The modified decamer crystallizes§ in the A-form, the right-handed duplex geometry presumably preferred by an LNA–LNA duplex. The crystallographic model was refined¶ with simulated annealing and force field methods, using an initial orientation from Molecular Replacement.¶ The decamer duplex exhibits an average helical rise of 2.95 Å and the average values for helical twist and inclination are 31.2 and 17.8°, respectively. An overview of the crystal data and refinement parameters is shown in Table 1 and final electron density maps around LNA residues are depicted in Fig. 2.

The sugar conformations of the two locked thymines 6 and 16 are both C3′-endo (Fig. 3) and the respective values for the pseudorotation[17] angle P are 16.9 and 18.3° (calculated with the program CURVES[18]). All deoxyriboses in the decamer exhibit C3′-endo puckers and the average value of their P angles (17.9°; excluding the two LNA residues) is very similar to those of the modified thymines. Thus, the bicyclic sugar moieties fit seamlessly into an A-form double helix and the additional restraints appear to lock them in an A-type pucker.

In addition to the sugar–phosphate backbone torsion angle δ that is a characteristic of the ribose conformation (Fig. 1), the five other backbone torsions adopt values that are also consistent with the standard sc^-, ap, sc^+, sc^+, ap, sc^- genus (α to ζ) of A-form double helices. A comparison of the backbone

Table 1 Crystal data and refinement parameters

Space group	orthorhombic $P2_12_12_1$
Unit cell constants [Å]	$a = 26.14$, $b = 43.96$, $c = 45.80$
Temperature [K]	110
Wavelength [Å]	0.93218
Beamline /detector	APS DND-CAT 5-ID/ MARCCD
Resolution [Å]	1.40
No. of unique reflections	10,950
Data completeness (all/last shell) [%]	99.7/96.7
R_{sym} (all/last shell) [%]	4.9/26.0
No. of nucleic acid atoms	408
No. of water molecules	127
R-work/R-free [%]	16.7/17.4
r.m.s for bonds/angles from standards Å/°	0.009/1.51
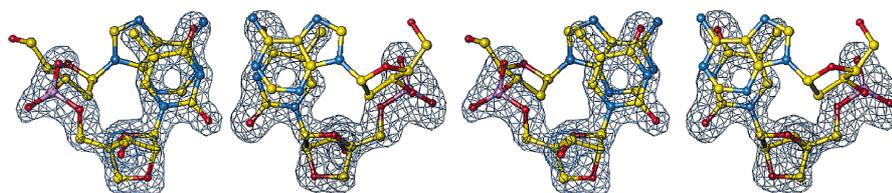
Fig. 2 Stereo drawing of the simulated annealing omit electron density (3σ-level) around modified residues T^{L}6 and T^{L}16 in the [(dA5pT^{L}6)- (dA15pT^{L}16] base pair step. Atoms are colored yellow, red, blue and magenta for carbon, oxygen, nitrogen and phosphorus, respectively.

torsions in the modified thymines with those in the rest of the duplex does not manifest any notable deviations. Therefore the bicyclic modification in LNA is fully compatible with the A-form geometry adopted by both DNA and RNA. Similarly, the glycosidic torsion angles in both LNA residues are in the standard *anti* geometry and no significant changes appear to result from the chemical modification in the local helical parameters, such as slide and x- and y-displacement (Fig. 3).

Our findings here based on X-ray crystallographic data are consistent with those obtained from NMR solution studies of DNA and RNA duplexes with either single or multiple LNA residues in one of the strands.[7–10] According to those experiments, the exceptional thermodynamic stability gains seen with LNA-modified duplexes (both in the DNA and the RNA contexts) are a result of the conformational preorganization of modified single strands for the duplex state (entropic contribution) as well as of the improved stacking both in the single- and double-stranded states (enthalpic contribution).

Unlike 2′-deoxyribose sugars which lack a functionality for hydrogen bond formation at the C2′-position, the locked sugars contain a hydrogen bond acceptor in the form of O2′ (Fig. 1). In the crystal structure both 2′-oxygens are engaged in hydrogen bonds to water molecules (Fig. 3). Extensive hydration of individual hydrogen bond acceptors and donors in oligonucleotides is often accompanied by an increased thermodynamic stability of the corresponding duplexes (see, for example, references 19 and 20). However, it is difficult to draw conclusions as to the role of sugar hydration in the overall stability of LNA-modified DNA duplexes or all-LNA duplexes. The arrangement of water molecules around locked sugars observed here is reminiscent of the solvation in the case of the 2′-oxygen in 2′-*O*-methyl RNA.[21,22] Duplexes of 2′-*O*-methylated oligoribonucleotides exhibit thermodynamic stabilities that are increased by about 1 °C per modified residue relative to RNA. However, the precise contribution of hydration to the stability increase in the case of 2′-*O*-methyl RNA is not understood.

Our study provides a first look at the conformational properties of LNA in a crystal structure at relatively high resolution. The main characteristics of the structure are the standard A-type conformation induced by LNA residues and the capacity of the 2′-oxygen that is part of the bicyclic sugar framework to engage in a least two hydrogen bonds to water molecules. Circular dichroism spectra (CD) of LNA–LNA duplexes in solution indicated that such duplexes appear to adopt a conformation that closely resembles the A-form geometry of RNA–RNA duplexes. However, these spectra also manifested subtle differences between the two species (data not shown). The present analysis of a duplex with only a single LNA residue per strand does not provide any insight into potential conformational differences between LNA and RNA duplexes. Attempts to determine a crystal structure of a completely modified LNA–LNA duplex are underway.

Notes and references

† Coordinates and structure factors have been deposited in the Protein Data Bank (pdb code 1i5w).
‡ The decamer was synthesized on a 2 μmole scale and the trityl-on strand was purified by RP-HPLC (C4, triethylammonium acetate pH 7–acetonitrile). Following detritylation the unprotected oligonucleotide was HPLC-purified a second time and then desalted.
§ Crystallization conditions were screened with a commercial sparse matrix kit (Nucleic Acid Miniscreen, Hampton Research, Laguna Niguel, CA), using the hanging drop vapor diffusion technique. Crystals suitable for diffraction experiments were obtained under the following conditions: 2 μl of a 2.8 mM decamer solution (single strand) were mixed with 2 μl buffer solution (10% 2-methylpentane-2,4-diol (MPD), 40 mM sodium cacodylate pH 6, 12 mM spermine tetrahydrochloride and 80 mM potassium chloride) and equilibrated against 1 ml of a 35% (v/v) MPD reservoir solution. A crystal was mounted in a nylon loop and shock-frozen in liquid nitrogen. Diffraction data were collected on the insertion device beamline (5-ID) of the DuPont-Northwestern-Dow Collaborative Access Team at the Advanced Photon Source (APS), Argonne National Laboratory (Argonne, IL). A total of 300 frames at high and low resolution ranges were recorded and reflections were integrated and merged in the DENZO/SCALEPACK suite.[11] A summary of amount and quality of the data is given in Table 1.
¶ The structure of the LNA-modified decamer was determined by the Molecular Replacement method using an A-form search model and the program AMORE.[12] The initial model was refined with the program CNS[13] setting aside 10% of the reflections for calculating the free R-factor.[14] Standard bond lengths and angles constraints[15] were employed for the DNA portion of the model and the geometric parameters for LNA residues were calculated with the program CHEM3D (CambridgeSoft Corporation, Cambridge, MA). The individual duplex models and the resulting Fourier electron density maps were visualized with the program TURBO-FRODO[16] on Silicon Graphics computers. Final refinement parameters and average root mean square (r.m.s.) deviations for bonds and angles from standard values are listed in Table 1. CCDC 156032.

1 A. A. Koshkin, S. K. Singh, P. Nielsen, V. K. Rajwanshi, R. Kumar, M. Meldgaard, C. E. Olsen and J. Wengel, *Tetrahedron*, 1998, **54**, 3607.
2 J. Wengel, *Acc. Chem. Res.*, 1999, **32**, 301.
3 S. Obika, D. Nanbu, Y. Hari, J. Andoh, K. Morio, T. Doi and T. Imanishi, *Tetrahedron Lett.*, 1998, **39**, 5401.
4 S. K. Singh, P. Nielsen, A. A. Koshkin and J. Wengel, *Chem. Commun.*, 1998, 455.
5 S. K. Singh and J. Wengel, *Chem. Commun.*, 1998, 1247.
6 C. Wahlestedt, P. Salmi, L. Good, J. Kela, T. Johnsson, T. Hökfelt, C. Broberger, F. Porreca, J. Lai, K. Ren, M. Ossipov, A. Koshkin, N. Jacobsen, J. Skouv, H. Oerum, M. H. Jacobsen and J. Wengel, *Proc. Natl. Acad. Sci. U.S.A.*, 2000, **97**, 5633.
7 C. B. Nielsen, S. K. Singh, J. Wengel and J. P. Jacobsen, *J. Biomol. Struct. Dyn.*, 1999, **17**, 175.
8 M. Petersen, C. B. Nielsen, K. E. Nielsen, G. A. Jensen, K. Bondensgaard, S. K. Singh, V. K. Rajwanshi, A. K. Koshkin, B. M. Dahl, J. Wengel and J. P. Jacobsen, *J. Mol. Recogn.*, 2000, **13**, 44.
9 K. E. Nielsen, S. K. Singh, J. Wengel and J. P. Jacobsen, *Bioconj. Chem.*, 2000, **11**, 228.
10 K. Bondensgaard, M. Petersen, S. K. Singh, V. K. Rajwanshi, R. Kumar, J. Wengel and J. P. Jacobsen, *Chem. Eur. J.*, 2000, **6**, 2687.
11 Z. Otwinowski and W. Minor, *Methods Enzymol.*, 1997, **276**, 307.
12 J. Navaza, *Acta Cryst. A*, 1994, **50**, 157.
13 A. T. Brünger, Crystallography & NMR System (CNS), Version 0.9, Yale University, New Haven, CT, 1998.
14 A. T. Brünger, *Nature*, 1992, **355**, 472.
15 G. Parkinson, J. Vojtechovsky, L. Clowney, A. T. Brünger and H. M. Berman, *Acta Cryst. D*, 1996, **52**, 57.
16 C. Cambillau and A. Roussel, Turbo Frodo, Version OpenGL.1, Université Aix-Marseille II, Marseille, France, 1997.
17 C. Altona and M. Sundaralingam, *J. Am. Chem. Soc.*, 1972, **94**, 8205.
18 R. Lavery and H. Sklenar, *J. Biomol. Struct. Dyn.*, 1989, **6**, 655.
19 M. Egli, N. Usman and S. Portmann, *Biochemistry*, 1996, **32**, 3221.
20 V. Tereshko, S. Gryaznov and M. Egli, *J. Am. Chem. Soc.*, 1998, **120**, 269.
21 P. Lubini, W. Zürcher and M. Egli, *Chem. Biol.*, 1994, **1**, 39.
22 D. A. Adamiak, J. Milecki, M. Popenda, R. W. Adamiak, Z. Dauter and W. R. Rypniewski, *Nucleic Acids Res.*, 1997, **25**, 4599.

Fig. 3 The [T^LpdA]$_2$ base pair step viewed approximately along the helical axis. Atoms of the upper and lower base pairs are shown in yellow and gray, respectively. Atoms of the sugar–phosphate backbone are colored green, red and magenta for carbon, oxygen and phosphorus, respectively. Water molecules within hydrogen bonding distance of O2′ atoms from **T^L** residues 6 (left) and 16 (right) are drawn as cyan spheres and hydrogen bonds are drawn as thin solid lines with their lengths indicated.